Developmental Biology 427 (2017) 21–34

Contents lists available at ScienceDirect

Developmental Biology

journal homepage: www.elsevier.com/locate/developmentalbiology

Modelling asymmetric somitogenesis: Deciphering the mechanisms behind species differences

Renske M.A. Vroomans*, Kirsten H.W.J. ten Tusscher

Utrecht University, Padualaan 8, 3584 CH, Utrecht, The Netherlands

ARTICLE INFO

Keywords:
Somitogenesis
Left-right signalling
Computational modelling
Determination front
Segmentation clock
Presomitic mesoderm

ABSTRACT

Somitogenesis is one of the major hallmarks of bilateral symmetry in vertebrates. This symmetry is lost when retinoic acid (RA) signalling is inhibited, allowing the left-right determination pathway to influence somitogenesis. In all three studied vertebrate model species, zebrafish, chicken and mouse, the frequency of somite formation becomes asymmetric, with slower gene expression oscillations driving somitogenesis on the right side. Still, intriguingly, the resulting left-right asymmetric phenotypes differ significantly between these model species.

While somitogenesis is generally considered as functionally equivalent among different vertebrates, substantial differences exist in the subset of oscillating genes between different vertebrate species. Variation also appears to exist in the way oscillations cease and somite boundaries become patterned. In addition, in absence of RA, the FGF8 gradient thought to constitute the determination wavefront becomes asymmetric in zebrafish and mouse, extending more anteriorly to the right, while remaining symmetric in chicken. Here we use a computational modelling approach to decipher the causes underlying species differences in asymmetric somitogenesis. Specifically, we investigate to what extent differences can be explained from observed differences in FGF asymmetry and whether differences in somite determination dynamics may also be involved.

We demonstrate that a simple clock-and-wavefront model incorporating the observed left-right differences in somitogenesis frequency readily reproduces asymmetric somitogenesis in chicken. However, incorporating asymmetry in FGF signalling was insufficient to robustly reproduce mouse or zebrafish asymmetry phenotypes. In order to explain these phenoptypes we needed to extend the basic model, incorporating species-specific details of the somitogenesis determination mechanism. Our results thus demonstrate that a combination of differences in FGF dynamics and somite determination cause species differences in asymmetric somitogenesis. In addition,they highlight the power of using computational models as well as studying left-right asymmetry to obtain more insight in somitogenesis.

1. Introduction

The vertebrate body plan displays bilateral symmetry, for instance in the placement of limbs and cranial features; somitogenesis is one of the major hallmarks of this symmetry. The regular blocks of tissue patterned during somitogenesis later on give rise to the vertebrae, ribs and skeletal axial muscles. Somite pairs are generated periodically in an anterior to posterior direction from the presomitic mesoderm (PSM). The use of mathematical modeling has a long and rich tradition in the somitogenesis research field and has played a critical role in our understanding of the mechanisms underlying somite formation (Cooke and Zeeman, 1976; Hubaud and Pourquié, 2014). It is now generally accepted (but see Cotterell et al. (2015)) that periodic somite patterning arises from a so-called clock and wavefront mechanism (Cooke and Zeeman, 1976; Hubaud and Pourquié, 2014). In the posterior part of the PSM, a complex regulatory network with multiple negative feedbacks generates regular gene expression oscillations, called the somitogenesis clock (Palmeirim et al., 1997; Resende et al., 2014). The transition from temporal oscillations to spatial stripes is thought to be governed by the so-called determination wavefront, a morphogen gradient that extends from the posterior to the anterior (Aulehla and Pourquié, 2010). In the posterior, where morphogen levels are high, cells are maintained in an undifferentiated state and gene expression oscillations are supported. As cells progress towards the anterior, they experience lower and lower morphogen levels, which eventually allows them to differentiate and cease to oscillate. This process results in the periodic generation of pairs of somites flanking the notochord, with left and right somites being generated with identical timing and spacing.

* Corresponding author.
E-mail address: renske.vroomans@gmail.com (R.M.A. Vroomans).

http://dx.doi.org/10.1016/j.ydbio.2017.05.010
Received 28 September 2016; Received in revised form 10 May 2017; Accepted 10 May 2017
Available online 12 May 2017

This symmetry becomes essential during later developmental stages when parts of the left and right somites fuse to form the vertebrae, and disturbances of somite symmetry can have severely disabling consequences such as scoliosis (Pourquié, 2011).

The somitogenesis clock, like all biological processes, is inherently noisy (Jiang et al., 2000; Herrgen et al., 2010). Therefore, additional levels of control are necessary to coordinate the behaviour of individual cells to ensure sharply delineated, coherent boundary formation and generate precise left-right symmetry. The processes synchronising cells along one side of the notochord have been studied extensively. Experimental data demonstrate that Delta-Notch mediated cell-cell signalling synchronises directly neighbouring cells (Özbudak and Lewis, 2008; Soza-Ried et al., 2014), an effect well known from modelling studies on coupled oscillators (Morelli et al., 2009; Herrgen et al., 2010). In addition, modelling studies have elucidated the importance of cell-mixing for synchronised oscillations (Uriu et al., 2009) and of cell-sorting for coherent somite patterning (Hester et al., 2011). In contrast, the precise mechanism underlying left-right coordination has only been partly elucidated experimentally and have thusfar not been investigated using a computational approach.

During part of the somitogenesis process, the left-right signalling pathway is active to confer left- or right-handed identity to the distal lateral plate mesoderm from which internal organs such as the heart and liver are generated (Brent, 2005). This left-right signalling not only passes through Hensen's node (Kupffer's vesicle in zebrafish) and the posterior PSM, but als leads to a transient asymmetrical distribution of signalling molecules such as FGF, Delta-Notch and Wnt that are also involved in somitogenesis (Boettger et al., 1999; Raya et al., 2003, 2004; Krebs et al., 2003; Kawakami et al., 2005; Tanaka et al., 2005; Nakaya et al., 2005; Jacobs-McDaniels and Albertson, 2011; Huang et al., 2011; Kato, 2011). Given the symmetry of somitogenesis this implies that under normal conditions compensatory mechanisms act to counteract the effects of left-right signalling on somitogenesis.

Experiments indicate that retinoic acid (RA) normally buffers the effects of the left-right pathway on somitogenesis, as somite symmetry is perturbed when RA is inhibited while left-right signalling remains unaltered (Kawakami et al., 2005). Interestingly, in absence of RA the left side becomes delayed in chick, while the right side becomes delayed in zebrafish and mouse (Kawakami et al., 2005; Vermot and Pourquié, 2005; Vermot et al., 2005; Sirbu and Duester, 2006; Brent, 2005). A potential cause for this difference could be the observed difference in FGF8 dynamics in absence of RA. While in chick the FGF8 gradient remains symmetric, in zebrafish and mouse the gradient of FGF8 extends more anteriorly on the right. Since FGF8 is an important component of the determination front, this may explain the different observed delays. However, there also exist additional species differences in the genes taking part in the somitogenesis oscillator (Krol et al., 2011), and in the precise dynamics of somite determination (Akiyama et al., 2014; Niwa et al., 2011). In this study, we use a modelling approach to investigate the mechanisms underlying the different asymmetry phenotypes observed in zebrafish, chick and mouse. We build on well-established clock-and-wavefront models of somitogenesis that were previously applied to study the influence of noise, delays in cell-cell signalling and mixing on synchronised somitogenesis (Morelli et al., 2009; Ares et al., 2012), by incorporating the asymmetric slowing of oscillator frequency in absence of RA. We subsequently extend this model in a stepwise fashion with the experimentally observed species differences in wavefront dynamics and somite determination to investigate their importance for the different asymmetry phenotypes.

We demonstrate that a simple clock and wavefront mechanism combined with asymmetric oscillator frequency is sufficient to explain the chick asymmetry phenotype. However, incorporating the additional asymmetry in FGF8 wavefront observed in zebrafish and mouse is insufficient to robustly reproduce zebrafish and mouse asymmetric somitogenesis. We show that the additional incorporation of species specific differences in somite boundary patterning mechanism is necessary to robustly simulate zebrafish and mouse asymmetry phenotypes. An additional advantage of these model extensions is that they pattern somites in a block-like fashion and well before gene expression oscillations cease which more closely resembles experimental observations (Shih et al., 2015; Niwa et al., 2011) than the cell-by-cell fashion concurrent with ceasing of oscillations that is typical of most clock-and-wavefront models. With our model, we can explain the paradoxical delay of chick somitogenesis on the left, while oscillator frequency is slowest on the right, from the ensuing differences in somite size. Finally, our models suggest that rostro-caudal somite polarity may arise from the temporal sequence of within somite patterning that is dictated by the frequency profile, a prediction that can be experimentally tested.

2. Methods

2.1. Clock and wavefront model

We model the presomitic mesoderm (PSM) as a 2D strip of cells. In the posterior the cells form a single coherent tissue representing the posterior zone where cells are added to the PSM (Posterior Addition Zone, or PAZ), more anteriorly the cells form two strips of tissue flanking the notochord (Fig. 2A). Each individual cell is endowed with an internal oscillation clock that is represented by a simple sinusoidal phase oscillator, as described in Jaeger and Goodwin (2001), Morelli et al. (2009), Murray et al. (2011), Ares et al. (2012) (Fig. 2A). We ignore the influence of noise or cell-cell signalling that have been extensively investigated in previous studies (Morelli et al., 2009; Herrgen et al., 2010; Murray et al., 2011; Ares et al., 2012). We assume that at the tissue level, a spatial frequency profile dictates oscillation frequency as a function of position in the PSM. Following work from Morelli et al. (2009) we described the frequency profile as:

$$\omega(x) = \omega_{max} * \left(1 - \frac{1}{\sigma^n} * x^n\right) \quad (1)$$

where $\omega(x)$ is the frequency at a certain distance x away from the posterior end of the PSM (Fig. 2B). ω_{max} is the oscillation frequency of cells at the posterior end of the PSM, and σ is the length over which the frequency will drop to 0. Usually σ is taken to be the PSM length, unless otherwise indicated. Finally, n is the exponent that determines the nonlinearity of the frequency profile: the higher the exponent, the further anterior in the PSM the frequency will start decreasing and the steeper the slope will be. When cells stop oscillating (at position σ, the anterior end of the PSM), they memorize their phase and become incorporated into a (pre)somite. Morelli et al. (2009) demonstrated that a frequency gradient of this shape reproduces the experimentally observed narrowing of waves of gene expression as these move anteriorly.

Cells are continuously added at the posterior end of the PSM, and the oscillators of these new cells are assumed to obtain the phase and frequency of the cells already present there (Fig. 2A). The anterior wavefront of somite determination travels toward the posterior at the same speed as cells are added, so that the PSM maintains a constant size (Morelli et al., 2009). The frequency profile shifts along, so that cells experience a progressively lower oscillation frequency, until the wavefront passes and their phase becomes frozen (Fig. 2B). We adapt this model of somite formation as we go on to account for differences between animals in the next section.

2.2. Left-right differences

When we implement left and right differences, we change the frequency ω_0, and/or the extent of the frequency profile σ differently in the left and right PSM, which results in different behaviour for the left

and the right somites (Fig. 2C). Often, the left side is kept the same as the starting conditions, for reference. We always start the simulations with the same ω_0 and σ on the left and the right, then "switch on" the difference after a few somites have been formed. The asymmetry is then maintained until the end of the simulation, unless otherwise indicated.

2.3. Extended models

As a first step in extending the above-described model, we incorporate an explicit description of FGF/Wnt (morphogen, M) decay driven gradient dynamics (Aulehla and Pourquié, 2010), following a similar approach as used in earlier modeling studies (Chisholm et al., 2011; Jorg, 2015), and model how the resulting spatial morphogen gradient becomes translated into an oscillator frequency profile. Individual model cells contain a specific level of morphogen. This level is set to a constant value of 1. in the PAZ and slowly decays in all other cells in the PSM, yielding an exponential posterior-to-anterior gradient. The dynamics in each cell outside of the PAZ are:

$$\frac{dM}{dt} = -decay * M) \tag{2}$$

We do not include morphogen diffusion in our model.

Next, we describe the dependence of oscillator frequence $\omega_1(x)$ on morphogen level using the following equation:

$$\omega_1(x) = \omega_{max} * \frac{M(x)^2}{M(x)^2 + 1/\beta^2} \tag{3}$$

where $1/\beta$ determines at which morphogen concentration the frequency has decreased to half its value in the PAZ. This dependence of frequency on morphogen concentrations was chosen to have this shape for two reasons. First, we assume that oscillator frequency can not increase indefinitely with higher morphogen levels but instead should saturate. Second, by combining a function of this shape with an exponentially decaying morphogen gradient a frequency profile is generated that closely resembles the frequency profile applied in the baseline model, for which earlier work demonstrated that it recapitulates experimentally observed wave dynamics.

We implement the observed asymmetry in anterior extent of the FGF gradient by adjusting FGF/Wnt decay rate. We assume that the decrease in oscillation frequency in the right PSM arises independently of FGF/Wnt and we model it through a decrease in the maximum of the frequency profile. The rationale for this assumption is that an increase in FGF on the right as observed in zebrafish and mouse would be expected to have a speeding up, rather than slowing down, effect, which contradicts the asymmetric phenotype. Furthermore, other factors besides FGF/Wnt are known to affect oscillation frequency more strongly (Resende et al., 2010).

We adapt this extended model separately for zebrafish and mouse, adding species-specific details as described below.

2.3.1. Zebrafish model

Experimental data (Akiyama et al., 2014; Wanglar et al., 2014) suggest that PSM cells transition through a sequence of discrete states before transforming into a fully determined somite. Oscillating cells start out in a "pErk high, Tbx6 high" state in the posterior PSM. As FGF levels drop beyond a certain level a first wave of Her expression causes cells to transition to a "pErk low, Tbx6 high" state, pre-patterning the S-IV-S-V somite boundary. A next wave of Her expression causes cells to transition to a "pErk low, Tbx6 low". Subsequent waves of Her expression are likely to induce further, not yet characterised, transitions in gene expression demarcating further differentiation until the S0 stage is reached and a fully determined somite forms. It is only in this final stage that oscillations are observed to cease (Shih et al., 2015).

The inclusion of explicit FGF8 decay dynamics in our extended model automatically enables us to simulate transitions in cell behaviour as cellular FGF8 levels fall below a critical threshold. Since we do not explicitly model gene expression dynamics, but rather only simulate oscillator phase, we defined particular oscillator phases to represent the start ($sin(\phi_1) > 0.95$) and termination ($sin(\phi_1) < -0.95$) of a passing Her expression wave. In absence of data on additional stages, we only model the transition from the "pErk high, Tbx6 high" to the "pErk low, Tbx6 high" and subsequently to the "pErk low, Tbx6 low" stage, after which oscillations are assumed to cease. By skipping these less known additional stages of somite determination, in our model oscillations cease 3 clock cycles earlier than in reality. However, our model does capture that somite boundary formation precedes termination of oscillations. In summary:

Algorithmic 1.

```
if sin(φ1) > 0.95 then
  if cell == ErkHIGH, TbxHIGH then
    cell == ErkLOW, TbxHIGH
  end if cell == ErkLOW, TbxHIGH then
    cell == ErkLOW, TbxLOW
else if sin(φ1) < −0.95 and cell == ErkLOW, TbxLOW then
  ω1(x) = 0
```

2.3.2. Mouse model

In mouse, experimental observations from Niwa et al. (2011), Harima and Kageyama (2013) suggest that somite determination is driven by a two-oscillator system. It was shown that while oscillations in Notch signalling slow down as cells progress anteriorly, pErk oscillations maintain a constant frequency. While in the posterior Notch and pErk levels peak synchronously, in the anterior a phase difference arises allowing Notch levels to become high when pErk levels are low, thereby setting in motion somite boundary determination. To simulate mouse somite boundary dynamics we added a "global oscillator" to our model which oscillates with the same phase and frequency across the entire PSM, thus mimicking the experimentally observed pErk dynamics.

$$\omega_2(x) = \omega_{max} \tag{4}$$

In the PAZ region, we assume that this global oscillator cycles with the same angular frequency ω_{max} as the travelling wave oscillator, while setting it a quarter phase (-0.5π) behind to allow the first wave to travel for a full oscillation cycle. As above, since we do not explicitly model gene expression oscillations, we have to cast the experimental observation that somite boundary formation occurs when Notch levels are high and pErk levels are low in terms of specific phases of the frequency gradient and global oscillator. We simulate this in our model by imposing that when the global oscillator is in the "low" ($\sin(\phi_2) < -0.9$) part of its cycle, the region where the travelling wave oscillator is high ($\sin(\phi_1) > 0.9$) – and all the tissue anterior to this region – stops oscillating and are transformed into a somite. In summary:

$$\omega_1(x) = \begin{cases} 0 & \text{if } \sin(\phi_2) < -0.9 \text{ and } \sin(\phi_1) > 0.9 \\ \omega_{max} * \dfrac{M(x)^2}{M(x)^2 + 1/\beta^2} & \text{otherwise} \end{cases} \tag{5}$$

and

$$\omega_2(x) = \begin{cases} 0 & \text{if } \sin(\phi_2) < -0.9 \text{ and } \sin(\phi_1) > 0.9 \\ \omega_{max} & \text{otherwise} \end{cases} \tag{6}$$

In addition to the above requirements for somite patterning in the mouse model, we can incorporate a threshold FGF (morphogen) level above which somites cannot form despite pErk levels being low and Notch levels being high. This additional threshold effectively delays

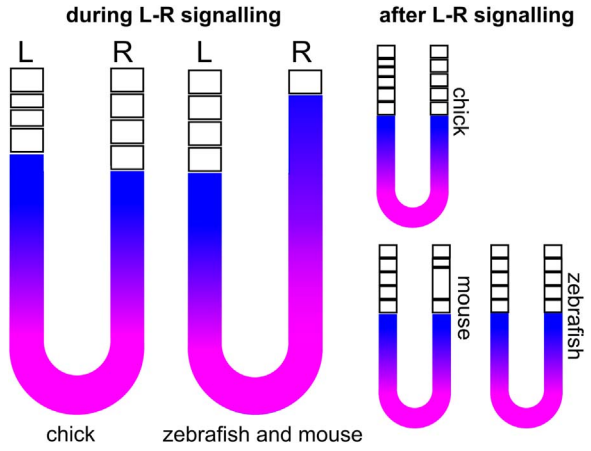

Fig. 1. Asymmetric somitogenesis phenotypes after RA knock-down. RA-inhibited chick embryos have symmetric FGF8 distributions and skewed somite formation, where the somites on the left are placed more anteriorly. Mice and zebrafish without RA instead have asymmetric FGF8 distributions and delayed somite formation on the right. While it is not entirely clear whether chick embryos return to symmetric somite formation, mouse and zebrafish embryos do. The difference between mouse and zebrafish is that in zebrafish, the "catch-up" somites (the somites that are formed more quickly to make up for the initial delay) are formed at symmetric positions compared to the left, while in mouse this is not always the case, and the catch-up region may even remain unpatterned.

somite formation and can lead to the formation of multiple travelling waves in the PSM. On top of this we can add a second, lower FGF threshold which works in the opposite direction: When the level of FGF in cells drops below this level, somite patterning ensues regardless of the phase of the global and travelling wave oscillators.

3. Results

3.1. A clock-and-wavefront model of somitogenesis

3.1.1. Chick, mouse and zebrafish differ in their asymmetric somitogenesis phenotypes

In chick embryos in which RA synthesis is inhibited chemically, the first 7 somites form normally but subsequent left-sided somites are formed more anteriorly than those on the right (Fig. 1). Oscillations slow down on the right (Vermot and Pourquié, 2005) (see Table 1), while the FGF8 gradient remains symmetric but extends more to the anterior, which is expected given the antagonistic interaction between FGF8 and RA (Diez del Corral et al., 2003).

In RA knock-out mice, after 9 symmetric somites have formed, somitogenesis becomes delayed in the right PSM by up to 3 somites. Furthermore, the travelling waves desynchronise between left and right and the FGF8 gradient is shifted more anteriorly on the right (Fig. 1). The delayed right-hand somites are often asymmetrically positioned, and occasionally the entire region remains unpatterned (Vermot et al., 2005). After left-right signalling has terminated, subsequent somites again form symmetrically.

Finally, in zebrafish with inhibited RA synthesis, the asymmetry looks similar to that in mouse, with a delay occurring between somites 6 and 13 in the right PSM. In contrast to mouse, the delayed right-side somites form at the same A-P position as the left, resulting in a fully symmetric spinal column at the end of somitogenesis (Kawakami et al., 2005) (Fig. 1, see also the Glossary).

3.1.2. Setting up the baseline model

We start with setting up an established clock-and-wavefront model (Morelli et al., 2009; Jaeger and Goodwin, 2001). Spatially, the model consists of cells forming a 2D tissue (the PSM), divided into a left and a right half located at either side of the notochord (Fig. 2A). At the posterior end, new cells are added at regular intervals, reflecting ingression and division; we call this region the Posterior Addition Zone (PAZ). In each cell, the somitogenesis clock is modelled as a phase oscillator. The experimentally observed slowing of oscillations towards the anterior of the tissue, thought to be caused by decreasing FGF and Wnt levels, is imposed by incorporating a frequency profile that dictates oscillation speed as a function of the distance from the posterior: $\omega(x) = \omega_{max} * (1 - \frac{1}{\sigma^n} * x^n)$ (Fig. 2B, see also Section 2). This frequency profile retracts at the same pace with which cells are added to the posterior end, resulting in a constant size of the PSM. The maximum frequency of the profile, which occurs in the PAZ, determines the pace of somitogenesis. Oscillations cease and somite

Table 1
Phenotypes of model organisms during somitogenesis.

genetic properties			left-right asymmetry in absence of RA					
organism	pErk dynamics	oscillating pathways	left-right phenotype	Slower osc	FGF8	delay (somite nr)	somite size diff	return to symmetry
chick	smoothly retracting	FGF, Wnt, Notch	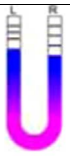	right side	symmetric, more anterior	no; left somites smaller	yes	unclear
zebrafish	retracts in jumps	Notch	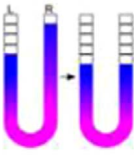	right side	right side more anterior	right side 2-3 somites delayed	no	yes
mouse	oscillates	FGF, Wnt, Notch	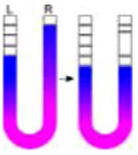	right side	right side more anterior	right side 2-3 somites delayed	sometimes	yes

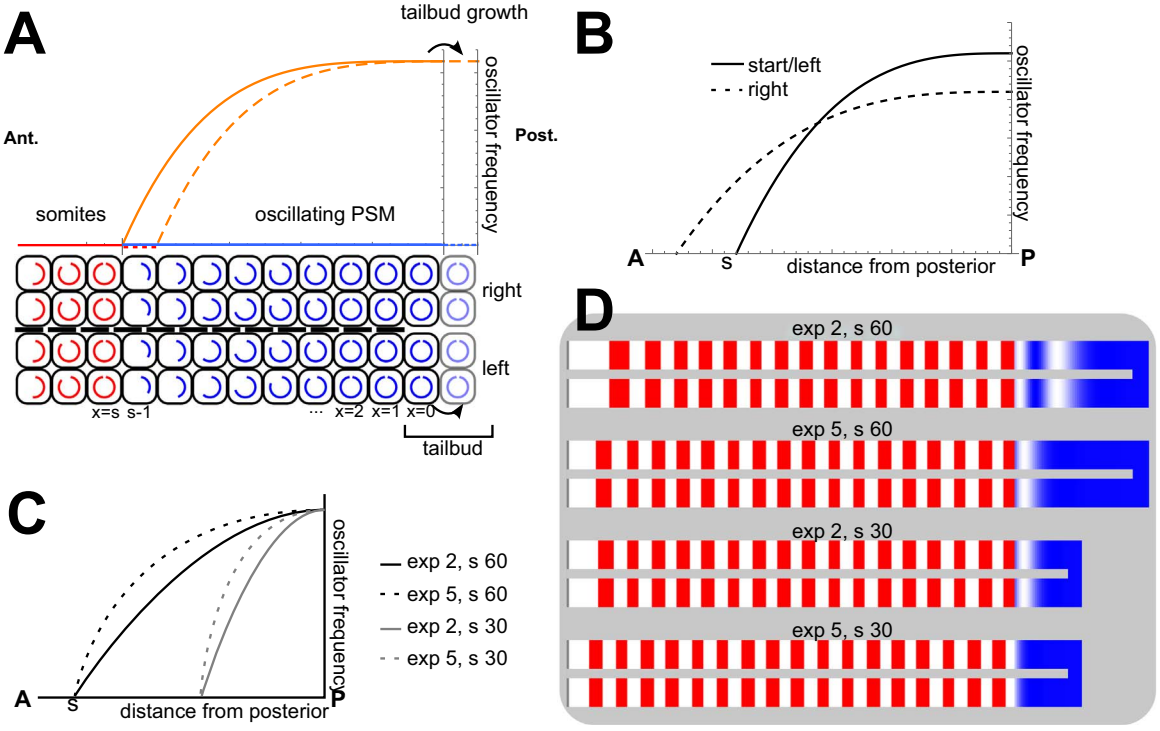

Fig. 2. A simple model of somitogenesis. A) We model a 2D tissue of cells with a phase oscillator (Morelli et al., 2009). The tissue is divided into a left and a right half. Cells are added to the PSM at the posterior end, (the Posterior Addition Zone, PAZ), and inherit the phase of the posterior-most cells. Above, we show the frequency profile (a negative quadratic function, see Section 2). The point at which the oscillation frequency becomes zero retracts at the same speed as the extension of the PSM in the posterior. The difference in frequency between cells in the posterior and more anterior cells results in a phase difference (the time of the clock, indicated by the coloured circles in the cells). In the region where somites are defined (indicated in red), cells no longer oscillate. B) An example of how the left and the right may differ in frequency profile. C) Different frequency profiles of the simulations shown in D, differing in steepness (exp) and extent (σ). D) The number of waves traversing the PSM for the different shapes of the frequency profiles. The separation between the left and the right halves in the figures is added later for clarity, and when waves are transformed to somites, we define the colours with a sharp cut-off for greater visibility.

patterning occurs at the point where the oscillation frequency becomes zero (σ), thus representing the determination front. Cells are assumed to memorize their current oscillator phase upon ceasing oscillations, and resulting spatial phase differences are assumed to pattern both somite boundaries and intrasomite polarity (Morelli et al., 2009) (Fig. 2D, Section 2). As has been shown before, the shape and length of the frequency profile determine the number of waves traversing the PSM: with a shorter and more nonlinear frequency profile, there are fewer travelling waves (Fig. 2C-D) (Morelli et al., 2009). This allows us to adjust the number of travelling waves to match the species being modelled.

3.1.3. Introducing asymmetry in clock frequency

Having established the baseline model, we now incorporate the observed asymmetry in oscillator frequency that is shared among chick, zebrafish and mouse when RA is absent. To mimick the fact that left-right signalling occurs in a limited time window of the entire somitogenesis process, we start simulations with symmetric left and right clock frequencies and wavefront positions, then at a certain time point impose the asymmetry in frequency between left and right (Fig. 2C). At a later timepoint, we may restore symmetric frequencies. A reduction in right oscillator frequency is modelled by lowering the maximum oscillation frequency on the right. We first investigate how to properly incorporate this asymmetry. Theoretically, two possibilities exist: either the left-right signalling pathway confers a frequency difference in the entire PSM, including the PAZ (Fig. 3B), or the difference in frequency only occurs anterior to the node, where left and right paraxial mesoderm are separated by the notochord (Fig. 3D). In Fig. 3A-B we show that when we incorporate the first possibility, the oscillation phase diverges between left and right in the PAZ, and the slower pace of oscillations on the right necessarily results in larger and fewer somites compared to the left (Fig. 3A-B). However, in experimental images we do not observe clear phase differences in the PAZ, suggesting that cells in the PAZ oscillate synchronously (Vermot and Pourquié, 2005; Vermot et al., 2005; Kawakami et al., 2005; Saúde et al., 2005). This absence of asynchrony in the left and right half of the tailbud may simply arise from the lack of physical separation in this part of the PSM. Previous studies have shown that both direct cell-cell signalling and cell mixing strongly homogenize oscillator frequency (Delfini et al., 2005; Uriu et al., 2010). Furthermore, left-right signalling occurs from Hensen's node (Komatsu and Mishina, 2013), which lies anterior to the PAZ and exerts its effect laterally. This would imply that the PAZ is not much affected by the left-right system. We therefore assume in all subsequent simulations that left-right asymmetry in oscillation frequency arises only in the non-PAZ region of the PSM (Fig. 3D). Our simulations show that this yields “phase forcing” of the oscillators in the right PSM, with the faster oscillations in the PAZ taking over control and driving the oscillation pace of the slower PSM. As a consequence, right-hand somites return to a size dictated by the PAZ frequency shortly after the left-right asymmetry is imposed (Fig. 3C). Because of the transition period in which the somites on the right were larger, somites on the right have become shifted posteriorly, resulting in fewer somites formed on the right (Fig. 3C).

3.1.4. The simple model accurately captures chick asymmetric somitogenesis

In experiments with chick embryos, inhibition of RA synthesis causes a symmetric anterior shift of the FGF8 gradient (Vermot and Pourquié, 2005), as may be expected from the known antagonism between RA and FGF (Diez del Corral et al., 2003). Given the role of FGF as the wavefront we incorporated this into our model as a symmetric anterior shift of the frequency profile that occurs simultaneously with the asymmetry in oscillator frequency. Upon termination of left right signalling frequency profiles are restored to initial,non-

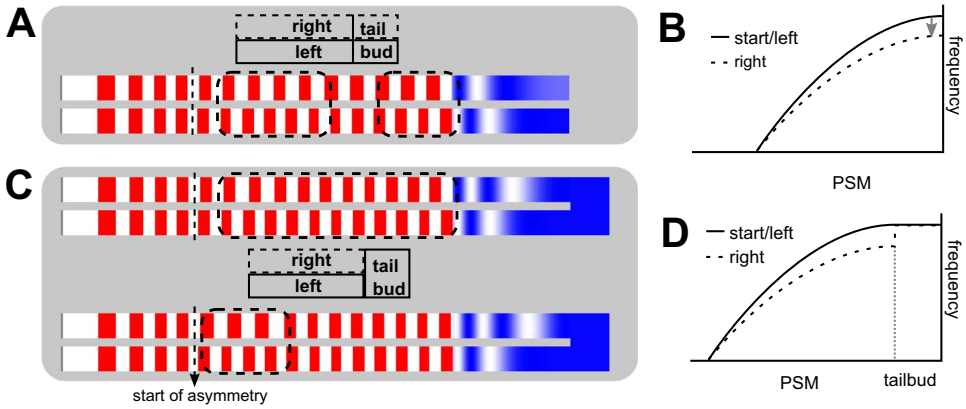

Fig. 3. Tailbud dynamics influence the course of asymmetric somitogenesis. A -B) Asymmetric frequency profile throughout the entire tissue (also PAZ, therefore the two halves are completely separated). The normal period is 90 min. At one third of the simulation, the period on the right side increases by 15 min. C-D) The PAZ is symmetric, the PSM is not. Top simulation: period on the right is 15 min longer. Bottom simulation: right period is 30 min longer. Regions with clear asymmetry are indicated with the boxes.

shifted and symmetric conditions. Addition of the anterior shift imposes a transient delay in somite formation, causing travelling waves to move anterior and continue narrowing longer (Fig. 4A, Video 1). This results in a number of smaller somites on both the left and the right as observed in experiments (Vermot and Pourquié, 2005; Vermot et al., 2005; Sirbu and Duester, 2006). However, the decrease in somite size is smaller on the right due to the simultaneously imposed lower oscillation frequency there, which on its own causes somite enlargement. These size differences cause an offset in left and right somite positioning. Thus, our model explains that the counterintuitive apparent delay of somitogenesis on the left (Brent, 2005) arises from the larger size of right-hand somites due to slower oscillations, combined with an anterior shift of the determination front, leading to smaller left sided somites during the early phases of left right signalling.

Later on, as PAZ frequency forcing sets in and left and right somites regain similar sizes it depends on the relative amount of oscillator slowing and frequency profile shifting whether or not symmetry already becomes restored while left-right signalling is still active (compare top and bottom panels in Fig. 4A). After termination of left-right signalling, a second opposite shift occurs restoring left-right symmetry. It is unclear whether this shift also occurs *in vivo*, and thus requires additional experimental validation.

3.1.5. Zebrafish and mouse asymmetric somitogenesis are more difficult to capture with the simple model

In order to simulate zebrafish or mouse somitogenesis, we need to take into account that the FGF8 gradient shifts more anteriorly on the right side, creating a larger oscillating region and a larger delay in somite formation on the right than on the left. To investigate the effect of an asymmetric shift in frequency profile in isolation, we initially only shift the frequency profile on the right, while keeping the left frequency profile and left and right oscillator frequencies constant (using mouse oscillator frequencies (period of 120 min) and somite size as an example; Fig 5A, left). We observe a delay in the formation of somites on the right (Fig 5A, right, top panel). Once the frequency profile shift is complete, one or more smaller somites are formed on the right (Fig. 5A left, bottom panel), causing an asymmetric positioning of all following somites.

Since in zebrafish (and occasionally in mouse) the “catch-up” somites are formed symmetrically, we investigate whether this asymmetric positioning of somites in our simulations can be avoided by incorporating the simultaneously occurring lower oscillation frequency on the right that would casue right sided somite enlargement (Fig. 5B, left, right). While certain combinations of left-right frequency difference and anterior shift allow us to generate symmetrically sized somites, we can not avoid an initial transient with asymmetric somites (Fig. 5B, left, lower panel). This may suffice to explain mouse somitogenesis, but in zebrafish the “catch-up somites” are formed at a symmetric position with the left side, which is now clearly not the case.

So far the decrease in oscillation frequency and anterior shift of the frequency profile were assumed to occur at the same time. When we instead assume that the oscillations on the right slow down before the profile starts to shift, we observe that the shift may compensate almost exactly for the increase in somite size that would otherwise ensue (Fig. 5C, right, top panel), although the first few somites on the right do remain a little larger. Notably, when the anterior shift is larger, also a larger decrease in oscillation frequency is required, otherwise the compensation does not suffice (Fig. 5C, right, bottom panel). Our simple model thus predicts that

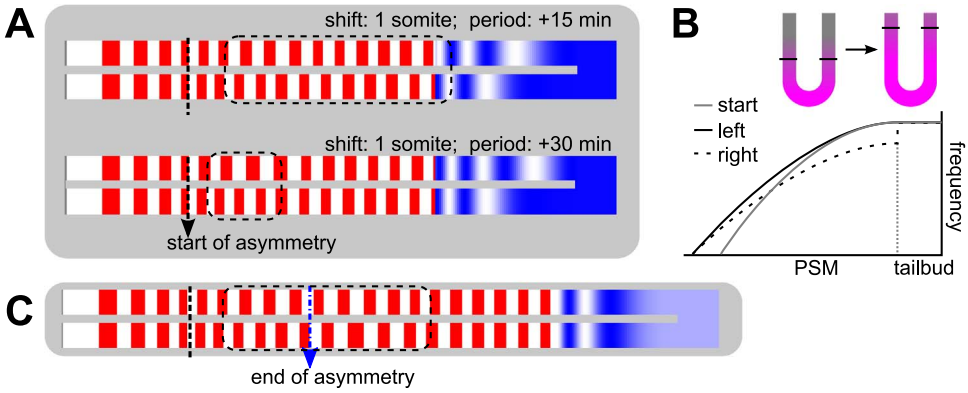

Fig. 4. The effect of a symmetric determination front shift during chick somitogenesis. A-B) Asymmetry combined with an anterior shift of the frequency profile (increase in σ, measured relative to normal somite size) on both sides. Left sided period is 90 min. C) Simulation in which at 2/3rd of the simulation, the frequency and determination front position are shifted back to normal values. Left period: 90 min, right period: 105 min, shift: 2 somites.

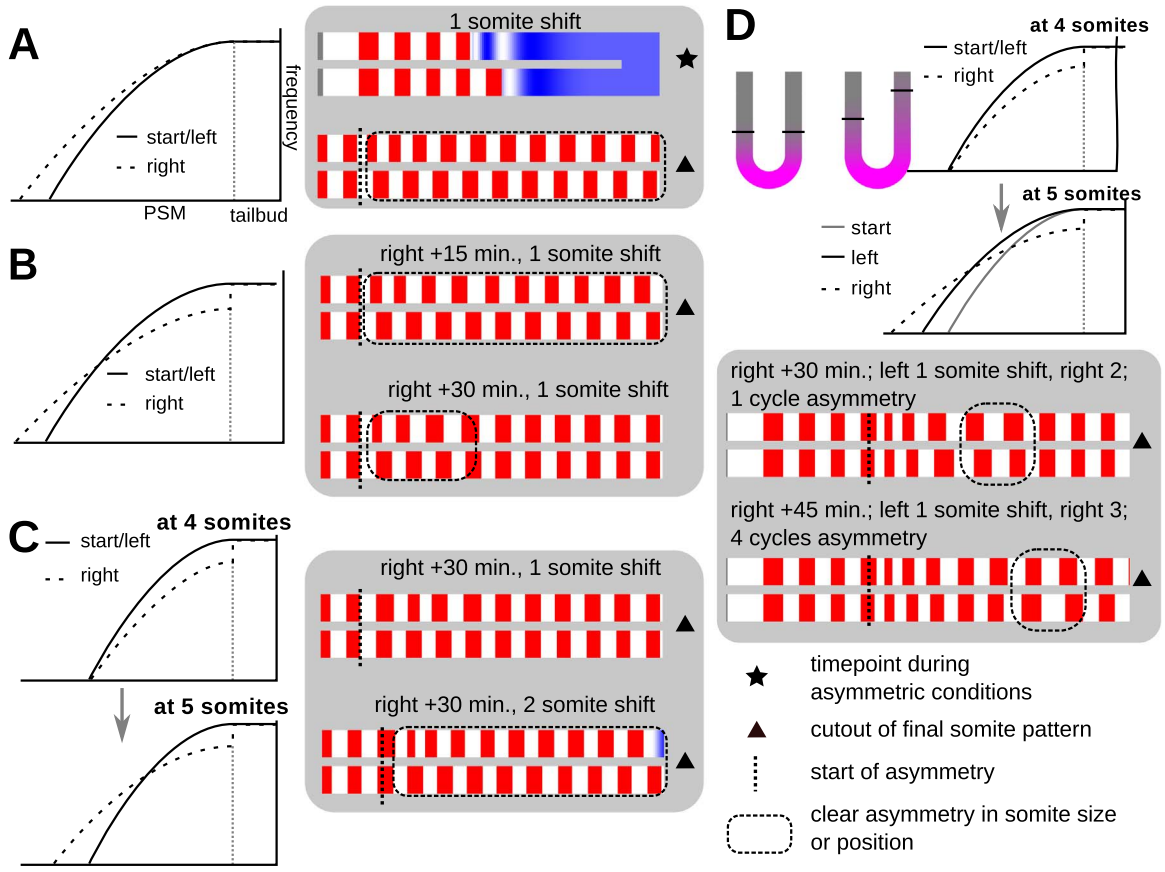

Fig. 5. The effect of an anterior determination front shift in the right PSM during mouse and zebrafish somitogenesis. A) Simulations in which only the extent of the frequency profile (σ) is increased on the right, at one third of the simulation. B) Simulations combining a drop in oscillation frequency on the right with the anterior frequency profile shift. C) Simulations in which the frequency drop comes one cycle before the anterior shift. D) Simulations in which the frequency profile also extends by one somite length on the left. Furthermore, after a number of cycles the conditions are restored to symmetrical values. Starting values: oscillation period=120 min, σ=60 cells. Values for the right PSM upon L-R signalling indicated in the figure.

in the right paraxial mesoderm of zebrafish, the frequency of oscillations should decrease prior to the anterior shift of the determination front to explain symmetric somite formation.

Finally, to completely mimic the experimental phenotype upon RA blocking, we need to also incorporate the lesser anterior shift of the left determination front as well as a return to symmetric parameters upon termination of left-right signalling (Sirbu and Duester, 2006). We find that under these conditions it becomes considerably harder to tune the size and timing of frequency difference, frequency profile shifts and return to symmetrical conditions (Fig. 5D, Video 2 and Supp. Fig. S1) to obtain symmetrically formed somites. We also repeated the simulations for zebrafish oscillator frequencies (period 30 min), and found that the tuning is equally difficult (Supp. Fig. S2). Thus, our simple model would imply that mouse and zebrafish asymmetry phenotypes are highly non-robust. Alternatively, while this model correctly reproduces chick asymmetric somitogenesis, it might be an incomplete representation of mouse and zebrafish somitogenesis. In the following sections, we will therefore re-evaluate some of the model assumptions, such as the smooth spatial transition from PSM to somite tissue and the transient halt of the progression of the determination front upon removal of RA, and adjust the model to better match experimental data on zebrafish and mouse.

3.2. Extended models of somitogenesis

3.2.1. Species differences in somite boundary establishment

Although the clock-and-wavefront model is widely accepted, the exact mechanism by which the oscillations are translated to a somite pre-pattern is still debated (reviewed in Hubaud and Pourquié (2014)). While there is evidence for a conserved role of boundary determination genes such as pErk, Mesp, Ripply and Tbx6 in zebrafish, chick and mouse (for review, see Yabe and Takada (2016)), there are also large differences in the number and type of oscillating genes between these species (Krol et al., 2011) (Table 1). For instance, while the pErk concentration profile smoothly retracts in chick, it displaces in discrete somite wide jumps in zebrafish, and oscillates in mouse (Akiyama et al., 2014; Niwa et al., 2011). Based on this we hypothesize that difference in wavefront and somite determination dynamics may play a role in species differences in asymmetric somitogenesis Table 2.

3.2.1.1. Zebrafish somitogenesis

3.2.1.1.1. Somite boundary formation through interactions between pErk, Tbx6 and Notch. Experimental data indicate that in zebrafish, somite boundary formation occurs already at somite S-IV Table 3. Spatiotemporal mapping data show that while the FGF8 profile retracts smoothly with the extending body axis, its downstream effector pErk is displaced by one somite length after each clock cycle (Akiyama et al., 2014). The resulting spatial transition from high to low pErk levels form the earliest sign of somite boundary patterning at somite S-IV. Interestingly, in a subsequent clock cycle the Tbx6 expression domain is also displaced posteriorly by one somite length (Wanglar et al., 2014). Notch oscillations appear involved in regulating this clock-wise retraction of pErk and Tbx6 expression (Akiyama et al., 2014; Wanglar et al., 2014). Oscillations continue up to somite S0, where somite morphogenesis takes place (Shih et al., 2015). At this point, oscillations have slowed to only 50% of the maximum frequency. It is likely that subsequent Notch cycles induce further transitions in gene expression involved in boundary formation and somite

Table 2
Outcome of different somitogenesis models for left-right asymmetry in different organisms.

Organism	Simple model	Zebrafish model	2 Oscillator model
chick	correct phenotype	n.a.	n.a.
zebrafish	yes, but hard to obtain symmetric formation of all somites −> have to tweak onset of different asymmetries.	yes; can obtain symmetric somites, natural origin of delay	n.a.
mouse	yes, but have to hard-code the delay on the right	n.a.	yes; natural origin of delay have to assume presence of two thresholds for somitogenesis. Asymmetric pErk dynamics more likely

differentiation (Shih et al., 2015).

3.2.1.1.2. Incorporating explict morphogen dynamics and somite boundary determination. To simulate these dynamics, we first replace the superimposed frequency profile with an explicit description of FGF/WNT morphogen gradient dynamics (as used before, (Chisholm et al., 2011; Jorg, 2015)), and how morphogen levels subsequently control oscillator frequency. Morphogen is produced in the PAZ and decays in other PSM cells following $\frac{dM}{dt} = -decay*M$, and morphogen levels determine oscillator frequency following $\omega_1(x) = \omega_{max} * \frac{M(x)^2}{M(x)^2 + 1/\beta^2}$ (for more details see Section 2). Combined, this generates a frequency profile similar to that of the simple model (Morelli et al., 2009) (Fig. 6A and Methods), yielding the characteristic narrowing of waves as they progress anteriorly.

Next, we decouple the frequency gradient from somite boundary determination, which should occur before rather than simultaneously with oscillation termination. A similar approach was followed in earlier modelling studies (Uriu et al., 2009; Jorg, 2015). We implement that when FGF8 morphogen levels fall below a certain threshold level, subsequent waves of Notch signalling (simulated as a certain phase of the oscillator) first repress pErk expression and then Tbx6 expression, and that only once a low pErk low Tbx6 state is reached oscillations cease and somite determination is complete (Fig. 6A,B) (for more details see Section 2). Based on the observation that Tbx6 switches on Mespa/b at the anterior boundary of its expression domain before retracting posteriorly (Wanglar et al., 2014), we define somite boundaries as cells having a distinct gene expression than their neighbors.

3.2.1.1.3. The model recapitulates P-A pErk and Tbx6 boundary displacement. In Fig. 6C we show simulations for normal, symmetric somitogenesis under different parameter settings. The top pictures show the phase of the oscillator in the PSM, while the bottom pictures show the cell states described above. We find that the number of travelling waves in the PSM can be increased by lowering the FGF8 threshold for gene expression state switching or by decreasing σ (which determines for which FGF8 level half the maximum frequency occurs). Both result in a larger PSM and cells at the anterior end of the PSM having a lower oscillation frequency (Fig. 6C, bottom). Decreasing the decay rate of FGF8 simply extends the PSM and increases the wavelength of the waves, but not their number (not shown). Notably, since somite determination occurs prior to the termination of oscillations in this model, somite polarity can no longer arise from memorization of oscillator phase as was the case in the baseline model. However, in our simulations, we observe that within an individual somite oscillations cease in a posterior to anterior manner, in agreement with experimental observations (Shih et al., 2015). This posterior-to-anterior progression of oscillation waves and their termination may provide time-dependent polarity information. Indeed, experimental data indicate that polarity establishment occurs later and downstream of boundary formation (Hubaud and Pourquié, 2014).

3.2.1.1.4. Frequency and wavefront changes have opposite effects. To simulate the anterior shift of FGF8 in the right PSM, we reduce the decay rate of the morphogen on the right after the formation of four somites, which leads to more FGF8 in the anterior PSM with some delay. We maintain symmetric oscillation frequencies and impose a return to symmetric decay values five cycles later. This yields a few smaller somites about three cycles after the introduction of the asymmetry, which creates the illusion of a delay on the right because the PSM extends further anteriorly, while the number of somites is the same (Fig. 7A). Upon return to symmetric values, a few oversized somites are formed that cause a return to symmetric somitogenesis. When instead the morphogen decay remains symmetric and only the frequency of oscillations is decreased on the right, somite formation there is truly delayed compared to the left. After four delayed but equally sized somites have been formed, somites on the right become larger than those on the left, so that somite formation becomes asymmetric (Fig. 7B). When the frequency on the right is returned to normal, a few smaller somites are created after which symmetry is restored. We thus observe that frequency decrease and FGF8 have opposing effects on somite size. Also note that the delay between gradient or frequency modification and effect on somitogenesis naturally follows from the predetermined somite states in the model, which means that a cluster of cells posterior to the last-formed somite

Table 3
Parameter values.

Parameter	Values	Remarks
clock-and-wavefront model		
chick ω_0	0.070 min^{-1}	maximum oscillation frequency in PAZ
mouse ω_0	0.052 min^{-1}	
zebrafish ω_0	0.21 min^{-1}	
chick n	2	exponent of quadratic equation governing frequency profile
mouse n	3	
zebrafish n	2	
σ	60 cells	length of frequency profile
zebrafish model		
normal ω_0	0.21 min^{-1}	asymmetric frequency values indicated in figure legends
normal FGF decay	0.005 min^{-1}	
FGF threshold for somite formation	0.15 a.u.	unless otherwise indicated
β	10	determines at which FGF concentration the frequency decreases
two-oscillator model		
mouse ω_0	0.052 min^{-1}	
chick ω_0	0.070 min^{-1}	
mouse n	2.5	
chick n	2	
normal FGF decay	0.005 min^{-1}	
β	10	determines at which FGF concentration the frequency decreases
FGF inhibitory threshold for somite formation	0.2 a.u.	
FGF forcing threshold for somite formation	0.05 or 0.075 a.u.	Slightly higher threshold required for chick simulations

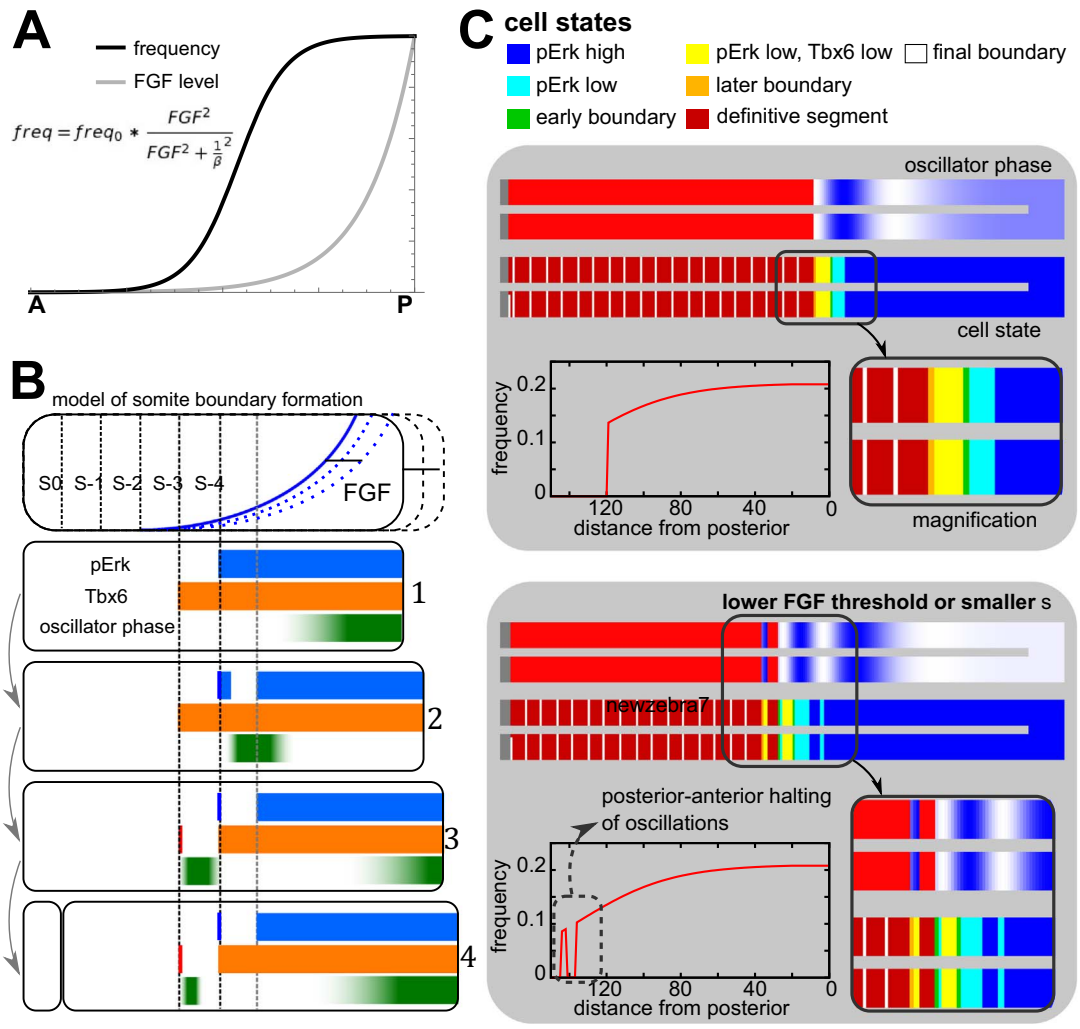

Fig. 6. A new model for zebrafish somitogenesis. A) Cells in the model have an explicit FGF8 level, which is 1 in the PAZ and decays with a fixed rate in cells in the PSM, mimicking the mRNA gradient. From this level, we derive the frequency of oscillations with the given equation. B) 1) Cells start in a so-called "pErk high, Tbx6 high" state in the posterior PSM (blue and orange bars both present). 2) After a cell's FGF8 level drops below a certain defined threshold (grey dotted line), it becomes competent to change to a "pErk low, Tbx6 high" state, which happens when they experience a peak in the oscillator phase ($sin(\phi) > 0.95$, phase indicated by the green bar). 3) When another peak passes, they transition to a "Tbx6 low" state (the orange bar disappears), which we for now consider to be the definitive segment state, upon which oscillations cease (4). For simplicity, boundary cells are defined as the last ones in a neighbourhood to transition to a new state, therefore switching on Mespa/b. Cartoon inspired by Wanglar et al. (2014), Saga (2012), Yabe and Takada (2016)) C) Examples of simulations with different σ (which determines at which concentration of FGF8 the frequency declines), or the FGF8 level at which cells can change to a 'pErk low" state.

already has determined somite boundaries and are unaffected by the change.

3.2.1.1.5. Tuning changes in oscillation frequency and FGF decay enables symmetric somitogenesis. When both frequency and decay rate are reduced on the right (and returned to normal after five cycles), there are combinations of decay rate and frequency change that yield delayed somite formation (lagging behind 2–3 somites) which subsequently becomes restored into symmetric somitogenesis, in agreement with experimental data (Kawakami et al., 2005) (Fig. 7C, Video 3). With a larger difference in frequency, the change in decay rate should also be larger to ensure maintenance of symmetric somite sizes. Still, somitogenesis remains roughly symmetric even for decay rates diverging to about 10% from the "perfect" compensatory decay rate (Supp. Fig. S3).

3.2.1.1.6. Conclusion. Similar to the baseline clock-and-wavefront model, our extended zebrafish model predicts the need to coordinate changes in oscillation frequency and wavefront position to obtain delayed but symmetric somitogenesis. However, in the extended model significantly less precise tuning was needed. In addition, while in the baseline model we also needed to precisely time frequency and wavefront changes, in the extended model the FGF8 decay dynamics automatically cause a delay in the onset of determination front displacement. Finally, the extended model offers a more natural explanation for the delay in somite formation on the right: a combination of delayed FGF8 gradient retraction and a slower clock increases the time needed to change the state of already-competent cells. This in contrast to the baseline clock-and-wavefront model, in which we had to assume that the determination front maintained at a constant position for several cycles to reproduce a delay in somite patterning. catch-up somites:

3.2.1.2. Mouse somitogenesis

3.2.1.2.1. Boundary formation through interactions of two oscillators. During mouse embryogenesis, many components of the Wnt, FGF and Notch signalling pathway oscillate (Krol et al., 2011). Oscillations of the FGF8 effector pErk are thought to determine the pace of somitogenesis (Niwa et al., 2011; Harima and Kageyama, 2013)

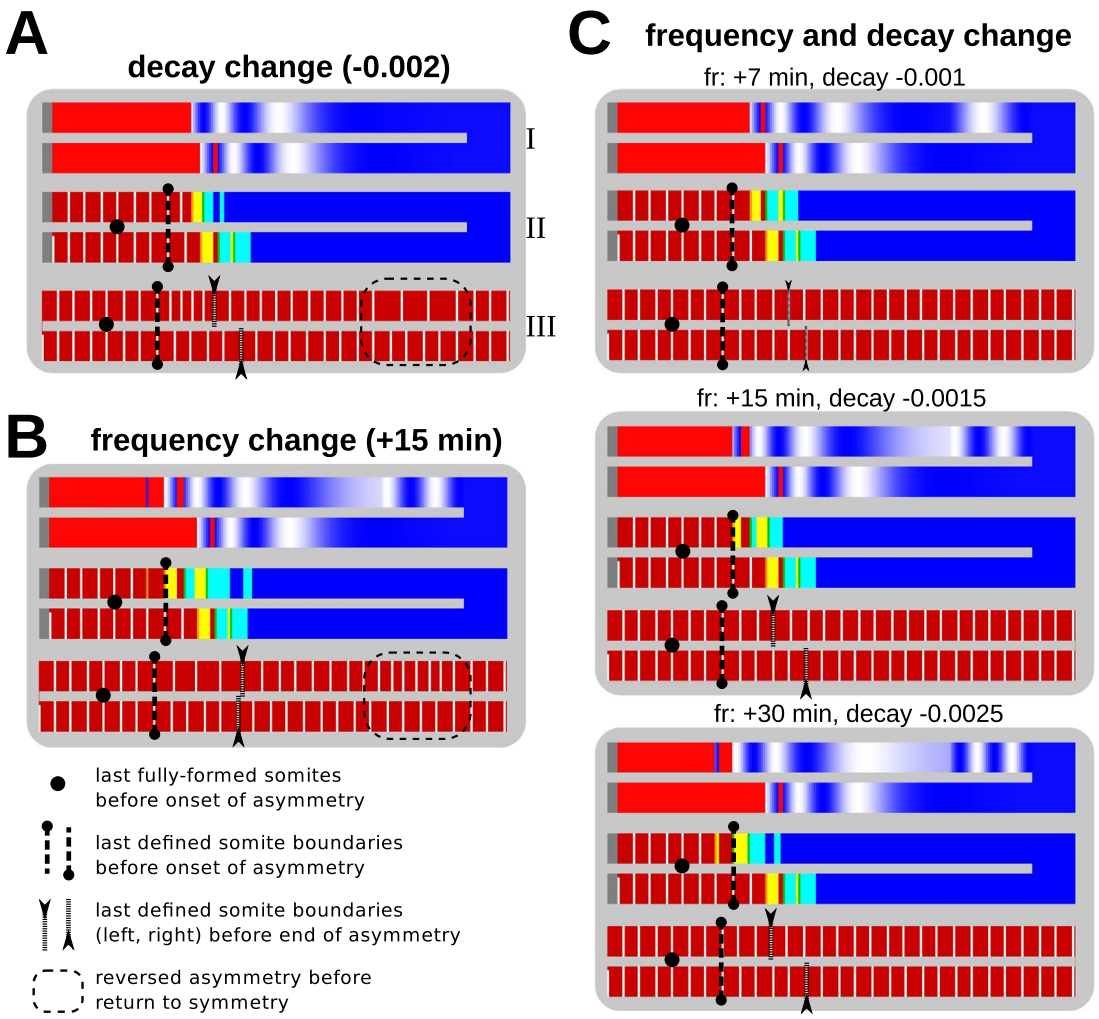

Fig. 7. Frequency change and FGF8 increase can compensate each other. Pictures display oscillation state during asymmetry (I), cell states during asymmetry (II) and all boundaries formed during the asymmetry period (III). The frequency changes and decay rate changes are for the right side only, starting at the 4 somite stage and ending at the 9 somite stage. Note the considerable delay between the change in parameters and a change in somite formation, due to the pre-emptively formed somite boundaries. In the right column, the change in frequency and decay are chosen such that symmetric somitogenesis is obtained, with never more than a one-cell shift in boundary position.

in mouse. It was shown that pErk oscillates approximately with the same period across the entire PSM, with a frequency similar to that of Notch in the PAZ (Niwa et al., 2011). As a consequence, in the anterior where Notch oscillations slow down, a frequency and hence phase difference arises between the two oscillators, allowing somite boundary formation to occur when Notch expression (travelling wave oscillator) is high while pErk expression is low. Boundary formation involves activation of Mesp2, which switches off Tbx6 and regulates somite rostro-caudal polarity (Oginuma et al., 2008; Yabe and Takada, 2016).

Although experimental data suggest that some coupling exists between Notch and pErk oscillators (Hayashi et al., 2009; Niwa et al., 2011), we simulate pErk oscillations as a "global" oscillator with a constant frequency (Fig. 8A): $\omega_2(x) = \omega_{max}$, that functions independently from the travelling wave (Notch) oscillator. In the PAZ the two oscillators are set to have the same frequency. To simulate somite formation, we defined a phase of the traveling wave oscillator as representing high Notch levels and an opposite phase of the global oscillator as representing low pErk levels, with boundary formation occurring when in the anterior the two oscillators are in these two states simultaneously (Fig. 8A; for more details see Section 2). Morphogen dynamics and the resulting frequency profile were modeled as in the extended zebrafish model.

3.2.1.2.2. Under symmetric conditions, the model does not require morphogen thresholds for somite determination. First we validate somitogenesis dynamics generated by this model under normal, symmetric conditions. In Fig. 8C and D, top pictures show PSM, somites and somite boundaries, while bottom pictures show the phase of the Notch oscillator at the time of somite formation. Please note that the latter is merely for illustration purposes: we do not assume that this oscillator phase reflects the final rostro-caudal polarity of the somites. Indeed, differences in oscillator phase at the time of somite formation easily arise due to different frequencies in the anterior-most cells at the time of somite formation, indicating that this would not allow for robust polarity patterning (compare the two simulations in Fig. 8C).

In principle, this model does not need a threshold morphogen level to determine when and where somitogenesis can occur like the zebrafish model does, as this is driven by the phase difference that arises in the anterior between the two oscillators (Fig. 8B). Under these conditions, the frequency profile of the Notch oscillator determines the size of somites (Fig. 8C), and only a single peak of Notch travels across the tissue at any given time. However, experimental data suggest the presence of an additional wave of Notch initiating right before somite formation (Niwa et al., 2011). Incorporating an FGF8 threshold (above which somitogenesis is inhibited), allows for more than one peak to form because it delays the moment at which somites can be formed, thereby retaining multiple travelling waves in the PSM (Fig. 6C,

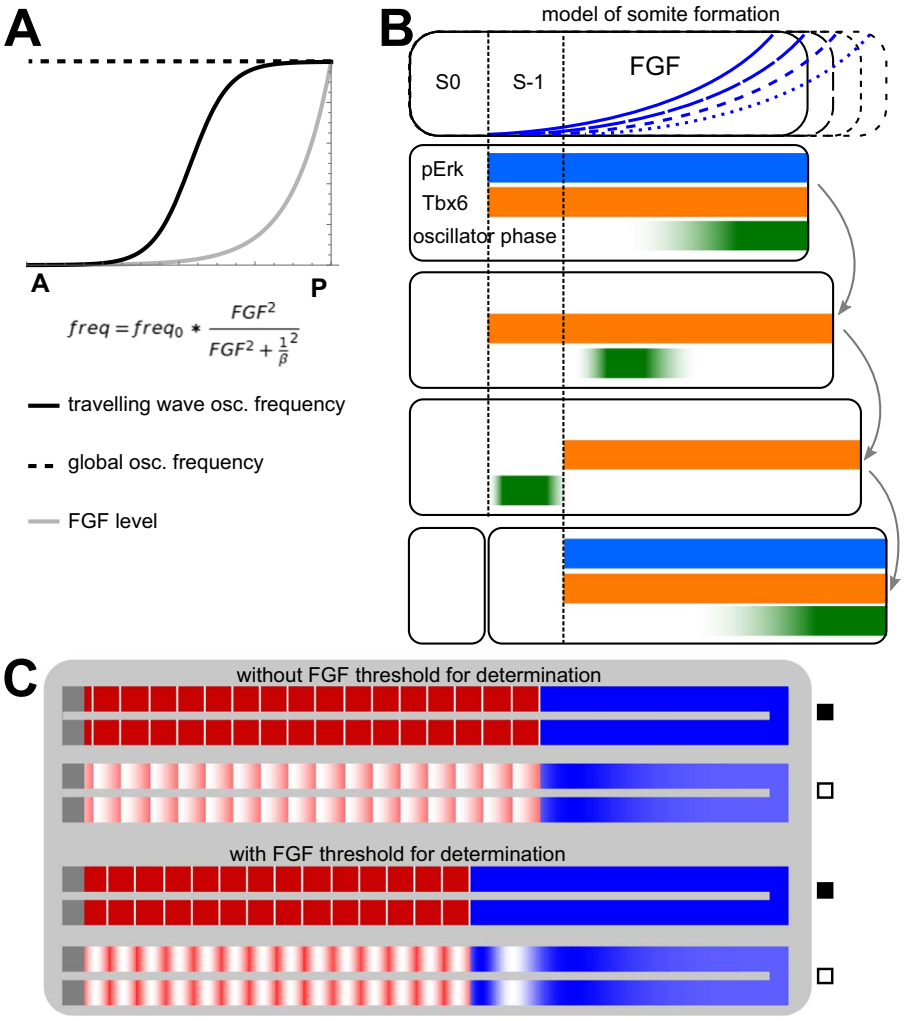

Fig. 8. The two-oscillator model. A) The frequency profile of the "global" pErk oscillations and the travelling-wave Notch oscillations. B) The formation and freezing of a wave in the two-oscillator model. The Notch oscillator forms a travelling wave towards the anterior, which creates a new somite when the pErk oscillation is at its minimum. We ignore somite polarity formation. Cartoon inspired by Saga (2012), Yabe and Takada (2016)). C) Examples of somitogenesis with the two-oscillator model. Filled squares indicate the image of cell state (blue, undifferentiated; red, differentiated somite; white, somite boundary), open squares indicate the image of oscillator phase, as before. First two rows: simulation without an FGF level threshold at which somitogenesis can take place. PAZ oscillation period: 120 min, σ: 10, FGF decay: 0.002, frequency profile exponent: 2.5. Last two rows: same parameters, but now with with an FGF level threshold at which somitogenesis can take place. threshold: 0.1 a.u.

Fig. 8C).

3.2.1.2.3. Unknown pErk dynamics in absence of RA. Having validated our extended mouse somitogenesis model for symmetric conditions, we now investigate whether it correctly captures asymmetric somitogenesis in absence of RA. However, while experimental data show that the domain of FGF expression extends further anterior in the right PSM (Vermot et al., 2005) and that the frequency of Her oscillations is decreased on the right, it is currently unknown whether or not pErk oscillations remain symmetric and with what frequency. We therefore decided to test two possibilities: either pErk oscillations remain symmetric with a frequency corresponding to the Notch oscillator frequency in the left PAZ, or pErk oscillations on the right become slower than on the left, with both sides having a frequency corresponding to the Notch oscillator in the PAZ at the respective sides.

3.2.1.2.4. Right sided delays are hard to explain for symmetric pErk oscillations. We first simulate symmetric pErk oscillations in the absence of an additional FGF8 gradient controlling somite formation. Under these conditions the symmetric pErk oscillation prevents delayed somite formation on the right, simply because the timing of somite patterning is fully determined by pErk dynamics. Asymmetry does arise from slower Notch oscillations producing a few very large somites on the right, followed by some very small somites after the symmetry in morphogen decay and Notch oscillation frequency is restored (Fig. 9A, top). Incorporation of the above discussed FGF8 threshold for somite formation allows for delayed somite formation on the right. The anterior extension of the right morphogen gradient (that occurs in absence of RA) causes somitogenesis to skip one or more cycles on the right, which in turn creates a sustained lagging of somitogenesis even upon return to symmetric parameter values (Fig. 9A, middle), inconsistent with experimental observations. If we make the additional assumption that below a certain morphogen level somite differentiation can no longer be prevented, we can incorporate a second lower morphogen threshold, which forces somitogenesis to happen regardless of the relative phases of the two oscillators. Incorporation of this second threshold resolves the persistent asymmetry by allowing the right PSM to catch up with the left (Fig. 9A, bottom, Video 4). Notably, the somites formed by the passing of the lower threshold are formed in a "non-canonical" manner: with a smoothly passing determination front defined by the threshold rather than in an oscillator dependent manner. This could potentially explain the aberrant determination of "catch-up" somites that is observed in some mouse embryos (Vermot et al., 2005).

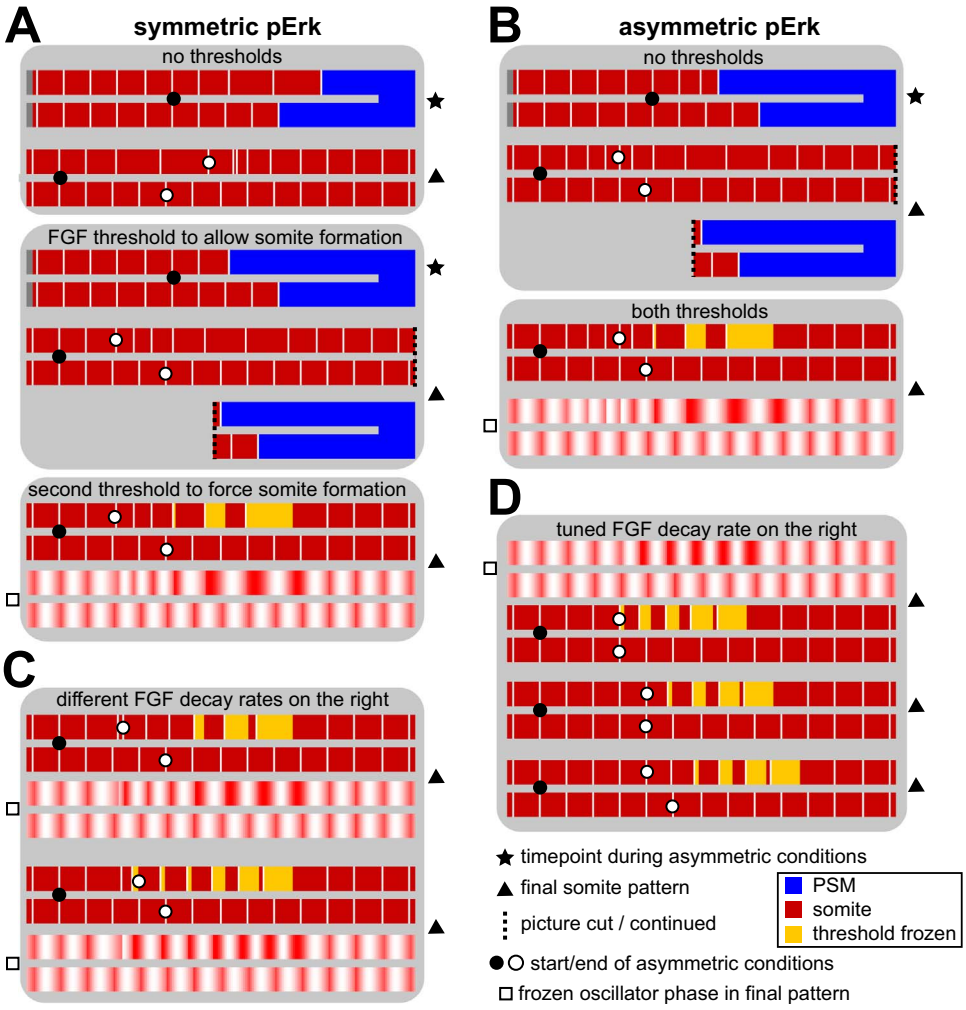

Fig. 9. FGF levels determining somite formation are required for correct reproduction of LR phenotypes. Most simulation images depict cell type, as specified in the legend; "threshold frozen" are the cells that stopped oscillating due to the passing of the explicit FGF threshold rather than the somitogenesis mechanism. For some simulations, the frozen oscillator phase is also shown (indicated with an open square). A) Simulations where pErk oscillations are symmetric. The first FGF threshold, restricting where somitogenesis can take place, is required to create a delay. The second threshold, a minimum FGF level required to keep cells in a non-determined state, is required to restore somite symmetry after frequency and FGF decay on the right have gone back to normal. B) Simulations where pErk oscillations are asymmetric. No thresholds are required to create a delay, but the minimum FGF level is required to restore symmetry. The threshold for somitogenesis has no effect (not shown here, identical phenotype to the top. Used parameters: normal period: 120 min, asymmetric period on the right: 150 min. Normal FGF decay: 0.005/min, right-hand FGF decay: 0.002/min; first threshold: 0.2 a.u.; second threshold: 0.05 a.u.; σ: 10; exponent: 2.5. Start of asymmetry after 6 formed somites, end after 4 more somites are formed on the left. C) Tuning the decay rate with symmetric pErk dynamics does not yield symmetric somite formation. FGF decay rates on the right: 0.003 and 0.004. D) Tuning the decay rate with asymmetric pErk dynamics can lead to delayed but symmetric formation of somites, except for altered polarity in the region where the catching-up mechanism has acted. The different rows have different durations of the asymmetric regime (3, 4 or 5 cycles). FGF decay is 0.004. See also Supp. Fig. S4 for tuning with larger frequency differences.

3.2.1.2.5. Asymmetric pErk oscillations naturally generate a right sided delay. If instead we assume that pErk oscillation frequency becomes asymmetric in absence of RA, the slower pErk oscillations naturally result in delayed somitogenesis on the right. Adding the first morphogen threshold for somite determination does not change this phenotype (not shown). However, again the delay persists upon return to symmetric conditions and a second lower morphogen threshold required to restore symmetry.

As in zebrafish, we can tune the morphogen decay rate such that somite formation is fairly symmetric, but only up to the point when the parameters are restored to symmetric values. Then, either the somites become irregular, or the passing of the lower threshold causes cells to stop oscillating regardless of the pErk and Notch oscillator phases, which again makes somite boundaries and polarity unclear (Fig. 9D, Supp. Fig. S4, Video 5). Note that such tuning of FGF8 decay and oscillator frequency asymmetry is impossible in the simulations with symmetric pErk, where some somites are always somewhat larger or smaller than on the left. Furthermore this cannot be improved by an additional tuning of the onset of morphogen decay asymmetry with respect to Notch frequency asymmetry, like we did with the simple model (Fig. 9C).

3.2.1.2.6. Conclusion. We suggest that asymmetric pErk dynamics may be more likely. First, experimental evidence indicates feedbacks from Notch to pErk oscillations (Hayashi et al., 2009; Niwa et al., 2011), making it likely that slower Notch oscillations lead to slower pErk oscillations. Secondly, our simulations show that for asymmetric pErk oscillations, the right sided delay in somite formation arises naturally from the right sided pErk slowing and does not lead to the skipping of one or a few rounds of somite formation. Independently of whether we simulate pErk oscillations asymmetrically or not, our model shows that consistent with experimental data the mouse

somite determination mechanism does not allow for the formation of fully symmetric catch-up somites. Thus our models suggest that the difference in asymmetry phenotype between zebrafish and mouse is caused by a difference in somite determination mechanism.

4. Discussion

A precise, reproducible and symmetric progression of somitogenesis is of crucial importance for vertebrate fitness, as evidenced by the severely disabling effects of conditions such as scoliosis. Still, although there is a rich tradition of developing models aimed at obtaining a better understanding of vertebrate somitogenesis, thus far models have not been applied for understanding left-right asymmetry. In the current paper we undertook the first steps in developing such models. In addition, we investigated the relevance of somite determination, the mechanism by which oscillations start to cease and somite boundaries are pre-patterned, for explaining the different left-right asymmetry phenotypes observed for different vertebrate model species.

In the current study we started out with a model in which the superimposed wavefront leads to oscillator stopping and phase memorization (Morelli et al., 2009). We also developed two new models. In the first, intended to mimic zebrafish somitogenesis, we incorporated the experimental observation that the early somite boundary marker pErk decreases its expression in discrete, somite wide jumps in a Notch oscillation dependent manner (Akiyama et al., 2014). With this model we show how a progressive delay can arise in somitogenesis in the right PSM following a decrease in oscillation frequency and an increase in the anterior extent of the wavefront, and how symmetry can be restored once left-right signalling terminates. This model reproduces the experimental observation that within an individual pre-somite, oscillations halt in a posterior-to-anterior manner (Shih et al., 2015). In addition it predicts a similar P-A progression for removal of pErk (and Tbx6 (Wanglar et al., 2014)) at the future somite boundaries, thus offering a potential explanation for the step-wise posterior shifts of the pErk domain boundary. More spatiotemporally resolved gene expression mapping will be needed to test whether this predicted P-A progression underlies the apparent jumps in pErk patterns.

In the second model, simulating mouse somitogenesis, we incorporated the experimental observation that pErk displays oscillations which do not slow with distance from the PAZ, and that somite boundary determination occurs when pErk levels are low, again in a Notch oscillation dependent manner (Niwa et al., 2011). Using this model, we show how the developing asymmetric phenotype depends on both the asymmetry in FGF levels as well as the assumed pErk dynamics in the delayed, right-hand PSM. If the pErk dynamics are also assumed to be slower in the right PSM, this model behaves similar to the zebrafish model, generating a progressive delay in right-hand somite formation. However, here this delay arises from the slowing of pErk rather than Notch oscillations. A difference between the zebrafish and mouse model is that while in the zebrafish model "catch-up" somites are formed with normal polarity information, this is not the case in the mouse model, which appears to be in agreement with experimental observations (Vermot et al., 2005). Furthermore, our mouse somitogenesis model predicts that catch-up somites form in a different manner than normal somites, independent of phase differences between the two oscillators and triggered by lower levels of FGF/Wnt signalling. This prediction could be experimentally validated by testing whether local FGF beads would prevent the formation of these catch up somites.

In the two new models, somite determination occurs without a memorization of oscillator phase. Since waves of Notch signalling set the pace of somite formation, somite determination occurs in a posterior to anterior manner, thus potentially providing alternative somite polarity information. Indeed, recently a two somite periodicity was observed to result from oscillator slowing and was proposed to contribute to the formation of sharply delineated somite boundaries and anterior-posterior polarity (Shih et al., 2015).

Note that our second model resembles another two-oscillator somitogenesis model, that was recently proposed to explain somite size scaling (Beaupeux and François, 2016). A notable difference between this model and the model we propose here is that rather than boundary determination arising from a particular size of the phase difference between the two oscillators, in our model determination occurs only if the two oscillators are simultaneously in a specific phase, as suggested by experimental data (Harima and Kageyama, 2013).

In vertebrates, the interactions between Wnt,FGF and RA determine the position of the determination front (Diez del Corral et al., 2003; Aulehla and Pourquié, 2010), and RA is involved in maintaining somite symmetry. Still, RA is not necessary for somite formation to occur. In amphioxus, the model species representative of the cephalochordate sister group of the vertebrates, somites form close to the PAZ and somitogenesis is asymmetric (Schubert et al., 2001). It was shown that FGF8 is not required for the formation of the posterior somites in amphioxus (Bertrand et al., 2011), FGF and RA do not interact (Bertrand et al., 2015) and RA is not able to generate symmetric somitogenesis. It thus appears that the FGF-RA antagonism evolved to ensure symmetric somitogenesis in vertebrates (Brent, 2005; Bertrand et al., 2011). Another striking difference between amphioxus and vertebrate somite formation is that in amphioxus somite determination occurs relatively close to the PAZ, whereas in vertebrates there is a large PSM between the PAZ and the determination front. This extended PSM may have arisen as a side effect of the evolution of the FGF-RA antagonism. Alternatively, the extended PSM may be essential to allow sufficient time and space for buffering small asymmetries and have been directly selected for. Clearly, much remains to be discovered on the function of the extended PSM, the PSM spanning oscillator frequency gradient and the resulting travelling waves for somite determination and symmetry.

Our study shows how differences in somite determination dynamics between the different vertebrate species may contribute to their diverse asymmetric phenotypes. Thus, the asymmetric phenotype arising in absence of RA provide additional information that can be used to further decode the underlying developmental mechanism. Indeed, our results suggest that rather than focussing on a catch-all mechanism in all vertebrate species and assuming that species differences merely reflect neutral developmental systems drift, we should keep an open mind for the possibility of functionally significant species differences.

Video 1. Simulation of asymmetric chick somitogenesis with basic model. After 5 oscillation cycles, the position of the determination front is shifted anteriorly by 2 somites on both sides. The oscillation period on the right is increased from 90 min. to 105 min. After 6 additional cycles (of 90 min.), the frequency and determination front position are shifted back to normal values. In all videos, anterior is at the top, and the position of the posterior end is fixed.

Video 2. Simulation of asymmetric mouse somitogenesis with basic model. After 4 oscillation cycles, oscillation period on the right is increased from 120 min. to 150 min. After another cycle (of 120 min.) the position of the determination front is shifted anteriorly by two somites on the right, and one somite on the left. When the wavefront shift is complete, the parameters return to symmetric values (after two cycles).

Video 3. Simulation of asymmetric zebrafish somitogenesis with extended model. After 20 oscillation cycles, the oscillation period on the right is increased from 30 min. to 45 min and the morphogen decay is decreased from 0.005 a.u. $min.^{-1}$ to 0.003325 a.u. min^{-1}. After 5 additional cycles these parameters are restored to normal values. The left image depicts the phase of the oscillator, the right image the cell states for the same simulation.

Video 4. Simulation of asymmetric mouse somitogenesis with extended model; symmetric pErk. After the formation of 1 small and 6 normal somites (10 cycles from the start of the simulation), the oscillation period on the right is increased from 120 min. to

180 min., and the morphogen decay is decreased from 0.005 to 0.002. After 4 cycles, these parameters are restored to normal values. Other parameters as in Fig. 9A, bottom. The left image depicts the phase of the oscillator, the right image the cell states for the same simulation.

Video 5. Simulation of asymmetric mouse somitogenesis with extended model; asymmetric pErk. After the formation of 1 small and 6 normal somites (10 cycles from the start of the simulation), the oscillation period on the right is increased from 120 min. to 150 min., and the morphogen decay is decreased from 0.005 to 0.004. After 5 cycles, these parameters are restored to normal values. Other parameters as in Fig. 9D, bottom. The left image depicts the phase of the oscillator, the right image the cell states for the same simulation.

Funding

This work was supported by NWO (Nederlandse Organisatie voor Wetenschappelijk Onderzoek), grant number [BB.000448.1 VIDI].

Acknowledgements

We thank Paulien Hogeweg and Enrico Sandro Colizzi for discussion and comments on the manuscript.

Appendix A. Supplementary data

Supplementary data associated with this paper can be found in the online version at http://dx.doi.org/10.1016/j.ydbio.2017.05.010.

References

Akiyama, R., Masuda, M., Tsuge, S., Bessho, Y., Matsui, T., 2014. An anterior limit of FGF/Erk signal activity marks the earliest future somite boundary in zebrafish. Development 141, 1104–1109.
Ares, S., Morelli, L.G., Jörg, D.J., Oates, A.C., Jülicher, F., 2012. Collective modes of coupled phase oscillators with delayed coupling. Phys. Rev. Lett. 108, 204101.
Aulehla, A., Pourquié, O., 2010. Signaling gradients during paraxial mesoderm development. Cold Spring Harbor Perspect. Biol. 2, 1–17.
Beaupeux, M., François, P., 2016. Positional information from oscillatory phase shifts: insights from in silico evolution. Phys. Biol. 13, 036009.
Bertrand, S., Camasses, A., Somorjai, I., Belgacem, M.R., Chabrol, O., et al., 2011. Amphioxus FGF signaling predicts the acquisition of vertebrate morphological traits. Proc. Natl. Acad. Sci. 108: 9160–9165.
Bertrand, S., Aldea, D., Oulion, S., Subirana, L., de Lera, A.R., et al., 2015. Evolution of the role of RA and FGF signals in the control of somitogenesis in chordates. PLoS One 10, e0136587.
Boettger, T., Wittler, L., Kessel, M., 1999. {FGF8} functions in the specification of the right body side of the chick. Curr. Biol. 9, 277–280.
Brent, A.E., 2005. Somite formation: where left meets right. Curr. Biol. 15, R468–R470.
Chisholm, R.H., Hughes, B.D., Landman, K.A., Mayer, G., Whitington, P.M., 2011. When are cellular oscillators sufficient for sequential segmentation? J. Theor. Biol. 279, 150–160.
Cooke, J., Zeeman, E., 1976. A clock and wavefront model for control of the number of repeated structures during animal morphogenesis. J. Theor. Biol. 58, 455–476.
Cotterell, J., Robert-Moreno, A., Sharpe, J., 2015. A local, self-organizing reaction-diffusion model can explain somite patterning in embryos. Cell Syst. 1, 257–269.
Delfini, M.C., Dubrulle, J., Malapert, P., Chal, J., Pourquié, O., 2005. Control of the segmentation process by graded MAPK/ERK activation in the chick embryo. Proc. Natl. Acad. Sci. USA 102: 11343–11348.
Diez del Corral, R., Olivera-Martinez, I., Goriely, A., Gale, E., Maden, M., et al., 2003. Opposing FGF and retinoid pathways control ventral neural pattern, neuronal differentiation, and segmentation during body axis extension. Neuron 40, 65–79.
Harima, Y., Kageyama, R., 2013. Oscillatory links of Fgf signaling and Hes7 in the segmentation clock. Curr. Opin. Genet. Dev. 23, 484–490.
Hayashi, S., Shimoda, T., Nakajima, M., Tsukada, Y., Sakumura, Y., et al., 2009. Sprouty4, an FGF inhibitor, displays cyclic gene expression under the control of the Notch segmentation clock in the mouse PSM. PLoS One 4, 1–8.
Herrgen, L., Ares, S., Morelli, L.G., Schröter, C., Jülicher, F., et al., 2010. Intercellular coupling regulates the period of the segmentation clock. Curr. Biol. 20, 1244–1253.
Hester, S.D., Belmonte, J.M., Gens, J.S., Clendenon, S.G., Glazier, J.A., 2011. A multi-cell, multi-scale model of vertebrate segmentation and somite formation. PLoS Comput. Biol. 7, e1002155.
Huang, S., Ma, J., Liu, X., Zhang, Y., Luo, L., 2011. Retinoic acid signaling sequentially controls visceral and heart laterality in zebrafish. J. Biol. Chem. 286, 28533–28543.
Hubaud, A., Pourquié, O., 2014. Signalling dynamics in vertebrate segmentation. Nat. Rev. Mol. Cell Biol. 15, 709–721.
Jacobs-McDaniels, N.L., Albertson, R.C., 2011. Chd7 plays a critical role in controlling left-right symmetry during zebrafish somitogenesis. Dev. Dyn. 240, 2272–2280.
Jaeger, J., Goodwin, B.C., 2001. A cellular oscillator model for periodic pattern formation. J. Theor. Biol. 213, 171–181.
Jiang, Y.J., Aerne, B.L., Smithers, L., Haddon, C., Ish-Horowicz, D., et al., 2000. Notch signalling and the synchronization of the somite segmentation clock. Nature 408, 475–479.
Jorg, D., 2015. Nonlinear transient waves in coupled phase oscillators with inertia. Chaos 25, 053106.
Kato, Y., 2011. The multiple roles of Notch signaling during left-right patterning. Cell. Mol. Life Sci. 68, 2555–2567.
Kawakami, Y., Raya, A., Raya, R.M., Rodríguez-Esteban, C., Belmonte, J.C.I., 2005. Retinoic acid signalling links left-right asymmetric patterning and bilaterally symmetric somitogenesis in the zebrafish embryo. Nature 435, 165–171.
Komatsu, Y., Mishina, Y., 2013. Establishment of left-right asymmetry in vertebrate development: the node in mouse embryos. Cell. Mol. Life Sci. 70, 4659–4666.
Krebs, L.T., Iwai, N., Nonaka, S., Welsh, I.C., Lan, Y., et al., 2003. Notch signaling regulates left-right asymmetry determination by inducing Nodal expression. Genes Dev. 17, 1207–1212.
Krol, A.J., Roellig, D., Dequéant, M.L., Tassy, O., Glynn, E., et al., 2011. Evolutionary plasticity of segmentation clock networks. Development 138, 2783–2792.
Morelli, L.G., Ares, S., Herrgen, L., Schröter, C., Jülicher, F., et al., 2009. Delayed coupling theory of vertebrate segmentation. HFSP J. 3, 55–66.
Murray, P.J., Maini, P.K., Baker, R.E., 2011. The clock and wavefront model revisited. J. Theor. Biol. 283, 227–238.
Nakaya, Ma, Biris, K., Tsukiyama, T., Jaime, S., Rawls, J.A., et al., 2005. Wnt3a links left-right determination with segmentation and anteroposterior axis elongation. Development 132, 5425–5436.
Niwa, Y., Shimojo, H., Isomura, A., González, A., Miyachi, H., et al., 2011. Different types of oscillations in Notch and Fgf signaling regulate the spatiotemporal periodicity of somitogenesis. Genes Dev. 25, 1115–1120.
Özbudak, E.M., Lewis, J., 2008. Notch signalling synchronizes the zebrafish segmentation clock but is not needed to create somite boundaries. PLoS Genet. 4, e15.
Oginuma, M., Niwa, Y., Chapman, D.L., Saga, Y., 2008. Mesp2 and Tbx6 cooperatively create periodic patterns coupled with the clock machinery during mouse somitogenesis. Development 135, 2555–2562.
Palmeirim, I., Henrique, D., Ish-Horowicz, D., Pourquié, O., 1997. Avian hairy gene expression identifies a molecular clock linked to vertebrate segmentation and somitogenesis. Cell 91, 639–648.
Pourquié, O., 2011. Vertebrate segmentation: from cyclic gene networks to scoliosis. Cell 145, 650–663.
Raya, A., Kawakami, Y., Rodríguez-Esteban, C., Büscher, D., Koth, C.M., et al., 2003. Notch activity induces Nodal expression and mediates the establishment of left-right asymmetry in vertebrate embryos. Genes Dev. 17, 1213–1218.
Raya, A., Kawakami, Y., Rodríguez-Esteban, C., Ibañes, M., Rasskin-Gutman, D., et al., 2004. Notch activity acts as a sensor for extracellular calcium during vertebrate left-right determination. Nature 427, 121–128.
Resende, T.P., Ferreira, M., Teillet, M.A., Tavares, A.T., Andrade, R.P., et al., 2010. Sonic hedgehog in temporal control of somite formation. Proc. Natl. Acad. Sci. 107: 12907–12912.
Resende, T.P., Andrade, R.P., Palmeirim, I., 2014. Timing embryo segmentation: dynamics and regulatory mechanisms of the vertebrate segmentation clock. BioMed Res. Int. 2014, 12.
Saúde, L., Lourenço, R., Gonçalves, A., Palmeirim, I., 2005. Terra is a left-right asymmetry gene required for left-right synchronization of the segmentation clock. Nat. Cell Biol. 7, 918–920.
Saga, Y., 2012. The mechanism of somite formation in mice. Curr. Opin. Genet. Dev. 22, 331–338.
Schubert, M., Holland, L.Z., Stokes, M., Holland, N.D., 2001. Three amphioxus Wnt genes (AmphiWnt3, AmphiWnt5, and AmphiWnt6) associated with the tail bud: the evolution of somitogenesis in chordates. Dev. Biol. 240, 262–273.
Shih, N.P., François, P., Delaune, E.A., Amacher, S.L., 2015. Dynamics of the slowing segmentation clock reveal alternating two-segment periodicity. Development 142, 1785–1793.
Sirbu, I.O., Duester, G., 2006. Retinoic-acid signalling in node ectoderm and posterior neural plate directs left-right patterning of somitic mesoderm. Nat. Cell Biol. 8, 271–277.
Soza-Ried, C., Öztürk, E., Ish-Horowicz, D., Lewis, J., 2014. Pulses of notch activation synchronise oscillating somite cells and entrain the zebrafish segmentation clock. Development 141, 1780–1788.
Tanaka, Y., Okada, Y., Hirokawa, N., 2005. FGF-induced vesicular release of Sonic hedgehog and retinoic acid in leftward nodal flow is critical for left-right determination. Nature 435, 172–177.
Uriu, K., Morishita, Y., Iwasa, Y., 2009. Traveling wave formation in vertebrate segmentation. J Theor Biol 257, 385–396.
Uriu, K., Morishita, Y., Iwasa, Y., 2010. Synchronized oscillation of the segmentation clock gene in vertebrate development. J. Math. Biol. 61, 207–229.
Vermot, J., Pourquié, O., 2005. Retinoic acid coordinates somitogenesis and left-right patterning in vertebrate embryos. Nature 435, 215–220.
Vermot, J., Llamas, J.G., Fraulob, V., Niederreither, K., Chambon, P., et al., 2005. Retinoic acid controls the bilateral symmetry of somite formation in the mouse embryo. Science 308, 563–566.
Wanglar, C., Takahashi, J., Yabe, T., Takada, S., 2014. Tbx protein level critical for clock-mediated somite positioning is regulated through interaction between Tbx and Ripply. PLoS One 9, 1–12.
Yabe, T., Takada, S., 2016. Molecular mechanism for cyclic generation of somites: lessons from mice and zebrafish. Dev. Growth Differ. 58, 31–42.